Optical model and coupled-channels analysis of ^{7}Li + ^{28}Si and ^{7}Li + ^{40}Ca scattering

John S. Eck
Department of Physics, Kansas State University, Manhattan, Kansas 66506

T. R. Ophel, P. D. Clark, J. Nurzynski, and D. C. Weisser
Department of Nuclear Physics, The Australian National University, Canberra, ACT 2600, Australia
(Received 30 November 1981)

Angular distributions for elastic scattering and for excitation of the 1.78 MeV state in ^{28}Si and for elastic scattering and excitation of the 3.73 and 3.90 states in ^{40}Ca by ^{7}Li scattering at a bombarding energy of 45 MeV have been measured and analyzed. Double folding model calculations using a realistic effective nucleon-nucleon interaction similar to that performed for ^{9}Be + ^{28}Si and ^{9}Be + ^{40}Ca scattering have been carried out for the elastic angular distributions and the real potential must be renormalized to yield agreement with the measured cross sections. Coupled channels calculations using a Woods-Saxon potential were performed in an effort to describe the inelastic angular distributions. The extracted deformation parameters are in reasonable agreement with those obtained from light and heavier ion scattering from the same target nuclei. The effect of strong excitation of the 0.48 MeV state in ^{7}Li and of mutual excitation of target and projectile is considered in a qualitative manner.

NUCLEAR REACTIONS ^{28}Si(^{7}Li,^{7}Li)^{28}Si, ^{28}Si(^{7}Li,^{7}Li*)^{28}Si* $Q=-0.48$, -1.78, and -2.26 MeV, $E(^{7}\text{Li})=45$ MeV; ^{40}Ca (^{7}Li, ^{7}Li)^{40}Ca, ^{40}Ca(^{7}Li, ^{7}Li*)^{40}Ca* $Q=-0.48$, -3.73, and -3.90 MeV, $E(^{7}\text{Li})=45$ MeV; measured $\sigma(\theta)$, $\theta_{\text{lab}}=10-70°$; performed optical model calculations using Woods-Saxon potential and double folding procedure, deduced optical model parameters; performed coupled-channels calculations, deduced deformation parameters.

There has been a great deal of recent interest in investigating the transition region between light projectile ($A \leq 4$) scattering and heavy projectile scattering ($A \geq 12$) from various target nuclei.[1-13] In particular, the scattering of ^{6}Li, ^{7}Li, ^{9}Be, and ^{10,11}B is presently being investigated in several laboratories and although a great wealth of data does not yet exist certain patterns are beginning to emerge. In particular, the double folding model using a realistic nucleon-nucleon interaction[14,15] which has been successful in describing the elastic α and heavy ion scattering from nuclei ranging in mass from $A=20\sim60$, is not successful in describing the elastic scattering of ^{6}Li, ^{7}Li, and ^{9}Be from the same target nuclei unless the real double folding potential is reduced by a factor of about $0.4\sim0.6$. Furthermore, the optical model using either the calculated double folding potential or one of Woods-Saxon shape indicates that the interaction separation for these transition nuclei is larger than for α and heavy-ion interactions with the same nucleus.[3-6] Perhaps more important is the transition from the dominance of the real potential to the dominance of the imaginary potential as we proceed through the transition region from α particle to ^{12}C scattering. In particular, the observation of nuclear rainbow scattering for ^{6}Li + ^{28}Si scattering is evidence for weak absorption in this case[2] while the lack of nuclear rainbow scattering and other evidence obtained from elastic and inelastic scattering and fusion studies of ^{9}Be with targets from the $A=20-60$ mass range indicate the dominance of strong absorption for ^{9}Be interactions.[1]

In order to investigate this transition in absorption strength, we have measured the elastic and inelastic scattering cross sections for excitation of the 1.78 MeV state in ^{28}Si, the 3.73 and 3.90 MeV states in ^{40}Ca, and the 0.48 MeV state in ^{7}Li using ^{7}Li projectiles at a bombarding energy of 45 MeV. In addition, the cross section for mutual excitation of the 0.48 MeV state in ^{7}Li and the 1.78 MeV state in ^{28}Si was measured. The experimental details are

given in Sec. II. The measured elastic cross sections were fitted using the same double folding procedure[14] that was successful in describing the elastic scattering of α particles and heavy ions ($A \geq 12$) and using an optical model potential of Woods-Saxon shape. The inelastic cross sections were fitted using the coupled channels code ECIS[17] and assuming that the low excited states of ^{28}Si can be described using a rotational model and the lowest states of ^{40}Ca can be described by a vibrational model. The calculations are described in Sec. III. Deformation lengths and deformation parameters are extracted from the fitted cross sections and compared with those obtained from measurements using other projectiles.[18,19] The effect of the absorptive potential on the calculated cross sections is investigated and compared to the dominance it exhibits in the case of ^{9}Be scattering from the same target nuclei.[1] These results are given in Sec. IV and the conclusions of this paper are given in Sec. V.

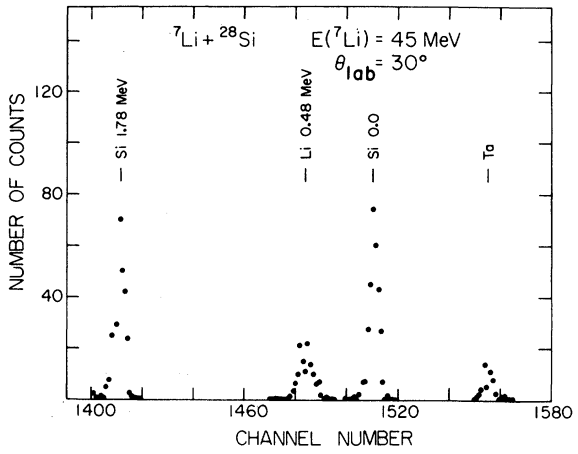

FIG. 1. Typical position spectrum gated on the ^{7}Li mass for ^{7}Li + ^{28}Si scattering at $\theta_L = 30°$ obtained using the Enge split pole spectrometer and focal plane detector.

EXPERIMENTAL

The ^{7}Li beam was extracted from a sputter source in the form of Li^- and was injected into the ANU 14UD tandem accelerator. The targets consisted of $\sim$200 μg/cm^2 self-supporting SiO_2 (greater than 99.5% enriched in ^{28}Si) or $\sim$160 μg/cm^2 Ca (greater than 99.8% enriched in ^{40}Ca) evaporated onto 10 μg/cm^2 C foils. The scattered ^{7}Li ions were detected using the Enge split pole magnetic spectrograph and focal plane detector which was operated in the light-ion mode.[20] By gating on the ^{7}Li mass, the states in ^{28}Si, ^{40}Ca, and ^{7}Li were clearly resolved up to about 7 MeV excitation energy. A typical spectrum for ^{7}Li + ^{28}Si is shown in Fig. 1. Because of the low Q values for the (^{7}Li, ^{6}Li) transfer reactions populating low-lying states of ^{29}Si and ^{41}Ca, the scattered ^{6}Li particles from the transfer reaction were also well focused on the focal plane of the dectector and, by gating on the ^{6}Li mass, the one-neutron transfer spectra were also obtained. The results of these measurements will be presented at a later time. The relative normalization was obtained by using a monitor detector placed at a laboratory angle of 15°. The absolute normalization was carried out by normalizing the measured cross sections to Rutherford scattering at a bombarding energy of 25 MeV and a laboratory scattering angle of 7.5°. The absolute normalization is accurate to $\sim$10%. The measured angular distributions are shown in Figs. 2—4. The elastic and inelastic angular distributions fall off quickly with in-

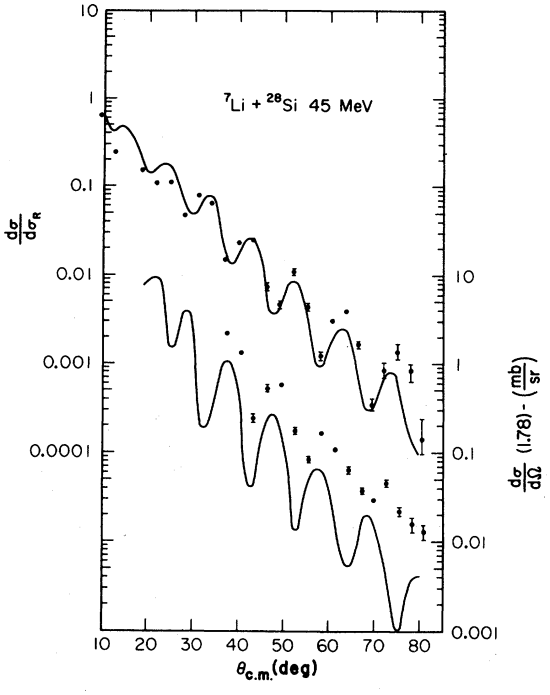

FIG. 2. Angular distributions for elastic scattering and inelastic scattering to the 1.78 MeV state of ^{28}Si by 45 MeV ^{7}Li projectiles. The elastic scattering cross section is shown as a ratio to the Rutherford by upper points. The inelastic cross section is given in absolute units and is indicated by the lower set of dots. The solid curves are cross sections calculated using the coupled channels code ECIS for the deformation parameter $\beta_2 = -0.15$. See text for details.

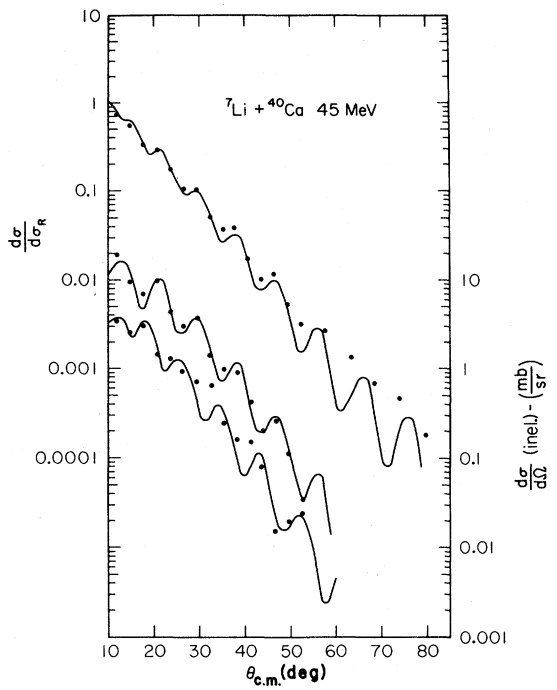

FIG. 3. Angular distributions for elastic scattering and inelastic scattering to the 3.73 and 3.90 MeV states of ^{40}Ca by 45 MeV ^{7}Li projectiles. Elastic scattering shown as a ratio to the Rutherford by the upper set of points. Inelastic cross sections for excitation of the 3.73 and 3.90 MeV states are given in absolute units and are indicated by the middle and bottom sets of dots, respectively. The solid curves are cross sections calculated using the coupled channels code ECIS for the deformation

creasing angle and show strong diffractionlike patterns. In the angular range measured ($10° < \theta_{c.m.} < 80°$), there is no indication of any leveling off or rising of the cross section with increasing angle[21,22] as has been observed for $^{12}C + ^{28}Si$ and $^{16}O + ^{28}Si$.

ANALYSIS

The elastic scattering angular distributions were fitted using a double folding model and a standard optical model of Woods-Saxon form. The double folding procedure used here is the same as that used elsewhere to describe ^{6}Li, ^{12,13}C, ^{14,15}N, and ^{16,17,18}O scattering from ^{28}Si, ^{40}Ca, and other nuclei in the same mass region.[14–16] The double folding potential may be written:

$$U_F(R)=\int d\vec{r}_1 \int d\vec{r}_2 \rho_1(r_1)\rho_2(r_2) \times V(r_{12}=R+\vec{r}_2-\vec{r}_1) ,$$

where ρ_i is the distribution of the centers of mass of the nucleons in the ground state of the ith nucleus, r is measured relative to the center of mass of nucleus i, and R is the separation distance between the centers of mass of the two interacting nuclei. The method for construction of the density distributions is given in detail in Ref. 14. The nucleon-nucleon effective interaction is based upon a G-matrix constructed from the Reid potential. The real folded potential $U_F(R)$ is constructed in the above manner and is multiplied by a normalizing factor N, where N is varied to obtain the best fit. A Woods-Saxon imaginary term with $R_w = r_w(A_t^{1/3} + A_p^{1/3})$ is added to give the total potential. In the present work r_w was fixed at a value of 1.3 fm. The normalization parameter for the real potential N, the imaginary potential strength W, and the diffuseness of the imaginary well a_w, are then varied to obtain the best fit. The best fit parameters are given in Table I and the best folding model fit calculations to the measured elastic scattering angular distributions are shown in Figs. 5 and 6. In order to fit the cross sections, it is necessary to renormalize the potential by a factor $N \approx 0.58$. This result is similar to that obtained for ^{6}Li and ^{9}Be scattering from the same target nuclei. It has been shown recently that the necessity for this renormalization is eliminated for the case of ^{7}Li and ^{9}Be scattering if quadrupole effects (and therefore reorientation) are included in the data analysis.[7] A difficulty with this approach is that it does not eliminate the necessity for renormalization of the potential for the case of ^{6}Li scattering.[14] A common property of these projectiles is their low binding energy and therefore an explanation of the renormalization in terms of this property might be suspected although this connection[12] is not well understood or well investigated.

Prior to carrying out the coupled channels calculations, the elastic scattering angular distributions were fitted using a Woods-Saxon potential of the form:

$$U(r)=\frac{-V_0}{1+\exp[(r-R_0)/a_0]} - i\frac{W_0}{1+\exp[(r-R_w)/a_w]} + V_c(r) .$$

The initial parameters were chosen to be those of Cramer *et al.*[23] used to fit $^{16}O + ^{28}Si$ scattering over a wide energy range. Only V_0 and W_0 were varied and the best fit parameters are listed in Table I and the calculated best fit cross sections are shown in Figs. 7 and 8 for ^{7}Li + ^{28}Si and ^{7}Li + ^{40}Ca, respectively. The ratio of the real to the imaginary poten-

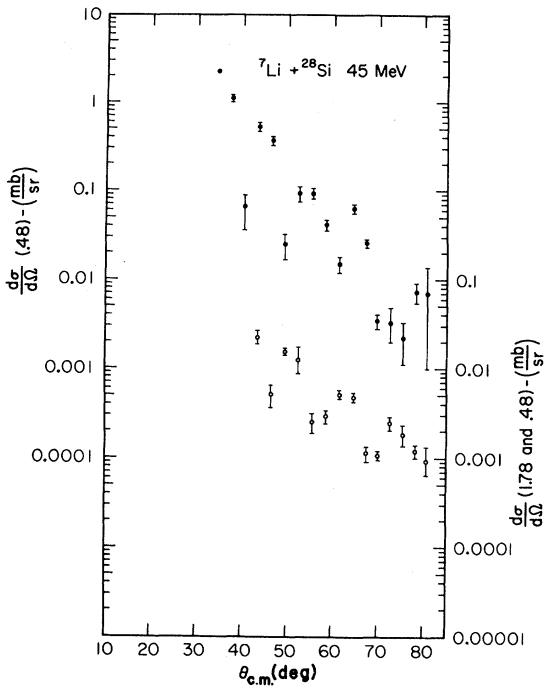

FIG. 4. Measured cross sections for excitation of the 0.48 MeV state of ^{7}Li (closed circles) and for mutual excitation of the 0.48 MeV state of ^{7}Li and the 1.78 MeV state of ^{28}Si (open circles) by ^{7}Li + ^{28}Si scattering at $E(^7\text{Li})=45$ MeV.

tial was calculated at $r=D_{1/2}$ where $D_{1/2}$ is the distance of closest approach for the Rutherford orbit for which $l=L_{1/2}$. $L_{1/2}$ is the value of l at which the transmission coefficient is $\frac{1}{2}$. The $D_{1/2}$, $L_{1/2}$ values and the ratio of W/V evaluated at $D_{1/2}$ are compared in Table I for the folding model calculation and the calculation involving the Woods-Saxon potential. The $L_{1/2}$ values are slightly different for each potential for both the ^{7}Li + ^{28}Si and ^{7}Li + ^{40}Ca scattering although the ratios of W/V indicate the dominance of strong absorption at $r=D_{1/2}$ in both cases.

The coupled channels calculations were performed using the computer code ECIS with 80 partial waves and radial integrations carried out to 40 fm to account properly for Coulomb excitation. The inelastic scattering for ^{7}Li + ^{28}Si was analyzed for 0^+-2^+ assuming a rotational model for the low-lying states of ^{28}Si and using quadrupole deformation only. The optical model parameters obtained from fitting the elastic cross section alone were utilized except that W was reduced on the order of 10% and the quadrupole deformation parameter β_2 was varied to obtain the optimal fit. The fits produced by this technique were not very satisfactory. The fit for $\beta_2=-0.15$ and $W=17.69$ is shown in Fig. 2. For these parameters the fit to the elastic cross section is good but that for the inelastic cross section is too low in magnitude and exhibits too much structure. Increasing the magnitude of the quadrupole deformation parameter to $\beta_2=-0.25$ improves the fit to the inelastic cross section but causes a deterioration in the elastic fit due to a reduction in the calculated diffraction structure, especially at back angles. This can be remedied slightly by decreasing W but then has the effect of increasing the calculated diffraction struc-

TABLE I. Best-fit optical model parameter sets. $L_{1/2}=l$ for which $T_l=\frac{1}{2}$ or $\eta_l=\sqrt{1/2}$. $D_{1/2}=$ distance of closest approach for Rutherford orbit with same $L_{1/2}$. $R_i=r_i(A_T^{1/3}+A_p^{1/3})$.

Target	N	W MeV	r_w fm	a_w fm	ρ_R mb	$L_{1/2}$	$D_{1/2}$ fm	-Re$U(D_{1/2})$ MeV	-Im$U(D_{1/2})$ MeV	Im/Re
Folding potentials										
^{28}Si	0.571	14.4	1.188	0.786	1688	21.5	8.0	0.68	0.91	1.33
^{40}Ca	0.586	13.6	1.241	0.795	1877	24.3	8.7	0.58	0.93	1.60

	V MeV	r_0 fm	a fm	W MeV	r_w fm	a_w fm	$L_{1/2}$	$D_{1/2}$ fm	-Re$U(D_{1/2})$ MeV	-Im$U(D_{1/2})$ MeV	Im/Re
Woods-Saxon potentials											
^{28}Si	7.17	1.35	0.618	17.69	1.20	0.552	20.55	5.95	5.27	9.943	1.89
^{40}Ca	7.96	1.35	0.618	19.26	1.20	0.552	22.74	6.84	4.69	8.29	1.77

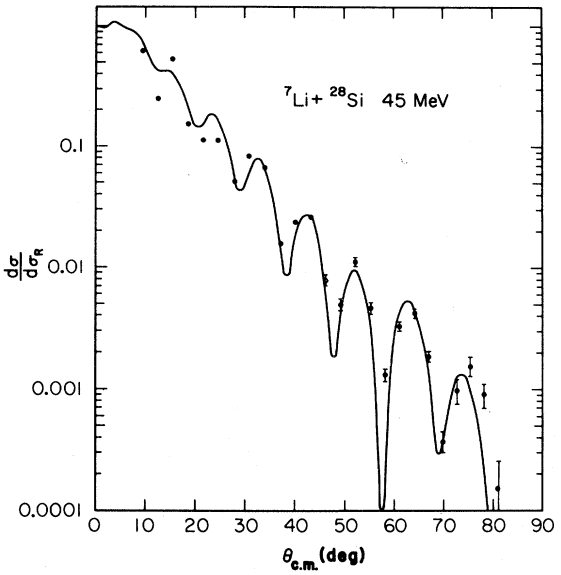

FIG. 5. Folding model calculation (solid curve) of ^{7}Li + ^{28}Si elastic scattering cross section at $E(^7\text{Li})=45$ MeV using the realistic nucleon-nucleon potential. See text for details. Experimental cross sections are indicated by closed circles.

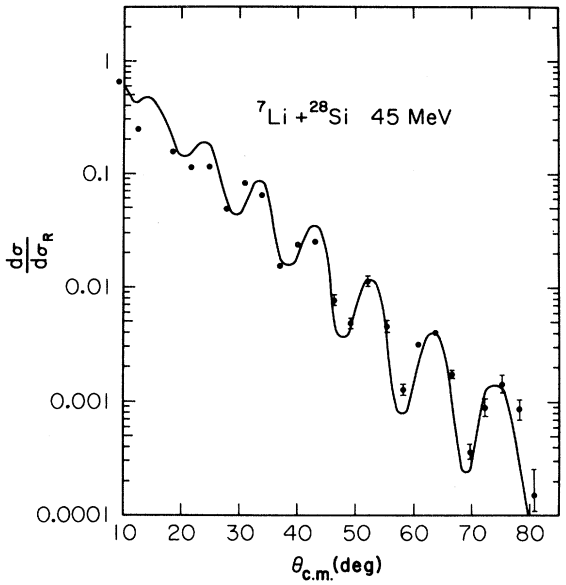

FIG. 7. Calculated angular distribution for ^{7}Li + ^{28}Si elastic scattering at $E(^7\text{Li})=45$ MeV using a Woods-Saxon potential and parameters of Table I.

ture in the elastic cross section beyond that which is observed in the measurements. The fit obtained for $\beta_2=-0.25$ and $W=15.00$ is shown in Fig. 9. A possible explanation for the poor quality fits is that the inelastic scattering to the 0.48 MeV state in ^{7}Li and the mutual excitation of the 0.48 and 1.78 MeV states are not included in the calculation. These cross sections are shown in Fig. 4 and comparison with Fig. 2 or 9 indicates that these neglected cross sections are similar in magnitude to the cross sec-

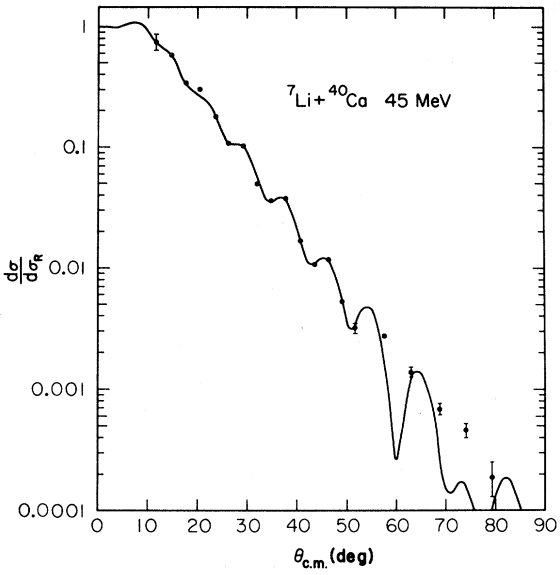

FIG. 6. Folding model calculation (solid curve) of ^{7}Li + ^{40}Ca elastic scattering cross section at $E(^7\text{Li})=45$ MeV using the realistic nucleon-nucleon potential. See text for details. Experimental cross sections are indicated by closed circles.

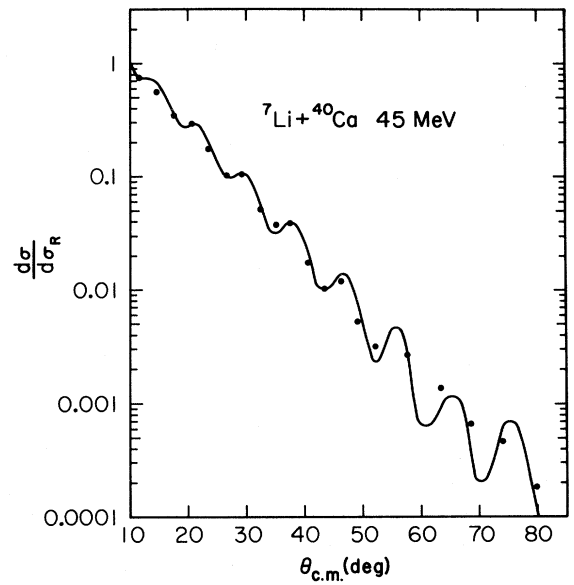

FIG. 8. Calculated angular distribution for ^{7}Li + ^{40}Ca elastic scattering at $E(^7\text{Li})=45$ MeV using a Woods-Saxon potential and parameters of Table I.

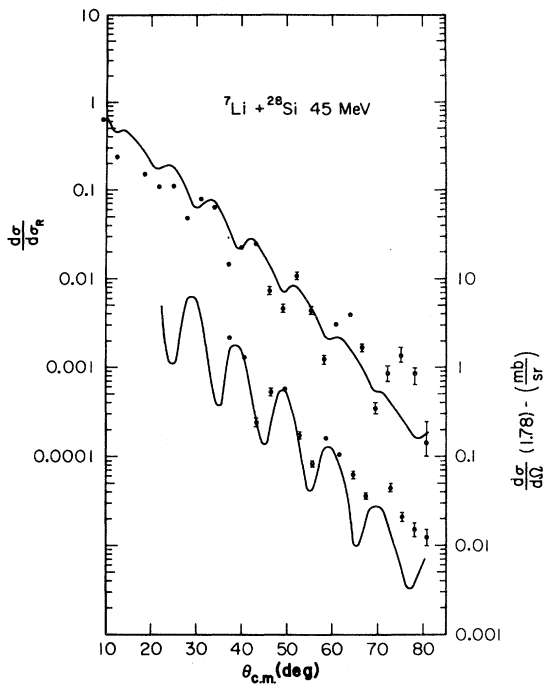

FIG. 9. Angular distributions for elastic scattering and inelastic scattering to the 1.78 MeV state of ^{28}Si by 45 MeV ^{7}Li projectiles. The elastic scattering cross section is shown as a ratio to the Rutherford by the upper set of closed circles. The inelastic cross section is given in absolute units and is indicated by the lower set of closed circles. The solid curves are calculated cross sections performed using the coupled channels code ECIS for the deformation parameter $\beta_2 = -0.25$. See text for details.

tion for exciting the 1.78 MeV state and need to be explicitly included in the coupled channels calculation if better results are to be expected. Unfortunately, this is presently beyond the capability of our coupled channels code.

The ^{7}Li + ^{40}Ca elastic and inelastic cross sections were fitted using a second order vibrational model to describe the low-lying 2^+ and 3^- states of ^{40}Ca. The 3.73 (3^-) state is assumed to be the excitation of one octupole phonon and the 3.90 (2^+) state is assumed to be the excitation of a single quadrupole phonon. By reducing W and adjusting β_2 and β_3 the fits shown in Fig. 3 were obtained. For this case $W = 18.00$, $\beta_3 = 0.15$, and $\beta_2 = 0.06$ and the fits are quite satisfactory. For ^{7}Li + ^{40}Ca the excitation of the 0.48 MeV state in ^{7}Li is again quite strong but not including it explicitly in the calculation does not appear to strongly affect the final fits. The values of β_3 and β_2 can be compared with those obtained from α particle scattering from ^{40}Ca at $E_\alpha = 29$ MeV by comparing the deformation lengths of the potentials in each case. The deformation length ρ_m is defined as

$$\rho_m = \beta_m R ,$$

where the potential radii from $\alpha + ^{40}$Ca and ^{7}Li + ^{40}Ca scattering used to obtain the deformation parameter fits are 4.76 and 7.20 fm, respectively. The deformation lengths are compared in Table II. Comparing the deformation lengths rather than deformation parameters yields better agreement between the two measurements as expected but there is still not a close agreement between these values.[18,19]

TABLE II. Deformation lengths for ^{40}Ca.

Experiment	$\beta_2 R$	$\beta_3 R$
$\alpha + ^{40}$Ca	0.57	1.19
^{7}Li + ^{40}Ca	0.43	1.80

CONCLUSIONS

The elastic and inelastic scattering cross sections for ^{7}Li scattering from ^{28}Si and ^{40}Ca targets have been measured and analyzed. The low-lying excited states of both target and projectile are strongly excited and in the case of ^{7}Li + ^{28}Si scattering mutual excitation of both target and projectile is significant. Folding model calculations of the elastic scattering cross sections yield potentials which must be renormalized by a factor of ≈ 0.6 in order to adequately fit the measured cross sections. Coupled channels calculations of the ^{7}Li + ^{28}Si scattering cross sections to the ground and first excited (1.78 MeV) state of ^{28}Si were not very well described by a simple rotational model description. A difficulty of the calculations reported here was the noninclusion of the excitation of the 0.48 MeV state in the coupled-channels calculation. In the case of ^{7}Li + ^{40}Ca scattering the cross sections for excitation of the ground, the first excited state (3^-) at 3.73 MeV, and the second excited state (2^+) at 3.90 MeV were fairly well described in the coupled channels calculations assuming a second order vibrational model. In this case, the 0.48 MeV state of ^{7}Li is again strongly excited but its noninclusion in the calculations does not seem to make any important differences in obtaining suitable fits. Comparison of the deformation lengths obtained here and those obtained from $\alpha + ^{40}$Ca scattering yield only rough

agreement. Suitable explanations of the differences observed in ^{7}Li scattering from both light and heavy ion scattering from the same nuclei have been put forth on the basis of the weak binding of ^{7}Li relative to the other projectiles and in terms of the reorientation effect due to the quadrupole moment of the ^{7}Li projectile but no single explanation so far has successfully explained all the observed differences in the measured cross sections by the intermediate projectiles ^{6}Li, ^{7}Li, ^{9}Be, and ^{10,11}B from those for light projectile $A \leq 4$ and heavy projectile ($A \geq 12$) scattering.

ACKNOWLEDGMENTS

The authors would like to thank S. Mukhopadhgay and G. R. Satchler for carrying out the folding model calculations reported here. This work was supported in part by the Division of Chemical Sciences, U. S. Department of Energy.

[1]M. S. Zisman, J. G. Cramer, D. A. Goldberg, J. W. Watson, and R. M. DeVries, Phys. Rev. C 21, 2398 (1980).

[2]R. M. DeVries, D. A. Goldberg, J. W. Watson, M. S. Zisman, and J. G. Cramer, Phys. Rev. Lett. 39, 450 (1977).

[3]R. Balzer, M. Hugi, B. Kamys, J. Lang, R. Müller, E. Ungricht, J. Untermährer, L. Jarczyk, and A. Strzalkowski, Nucl. Phys. A293, 518 (1977).

[4]E. Ungricht, D. Balzer, M. Hugi, J. Lang, R. Müller, L. Jarczyk, B. Kamys, and A. Strzalkowski, Nucl. Phys. A313, 3761 (1979).

[5]J. S. Eck, T. R. Ophel, P. D. Clark, D. C. Weisser, and G. R. Satchler, Nucl. Phys. A341, 178 (1980).

[6]J. S. Eck, T. R. Ophel, P. D. Clark, and D. C. Weisser, Nucl. Phys. A334, 519 (1980).

[7]V. Hnizdo, K. W. Kemper, and J. Szymakowski, Phys. Rev. Lett. 46, 590 (1981).

[8]C. W. Glover, K. W. Kemper, L. A. Parks, F. Petrovich, and D. P. Stanley, Nucl. Phys. A337, 520 (1980).

[9]C. W. Glover, R. I. Cutler, and K. W. Kemper, Nucl. Phys. A341, 137 (1980).

[10]M. F. Steedan, J. Coopersmith, S. J. Cartwright, M. D. Cohler, N. M. Clarke, and R. J. Griffiths, J. Phys. G 6, 501 (1980).

[11]R. I. Cutler, M. J. Nadworny, and K. W. Kemper, Phys. Rev. C 15, 1318 (1977).

[12]J. S. Eck, J. R. Leigh, T. R. Ophel, and P. D. Clark, Phys. Rev. C 21, 2352 (1980).

[13]K. Bodek, M. Hugi, J. Lang, R. Müller, E. Ungricht, K. Jankowski, W. Zipper, L. Jarczyk, A. Strzalkowski, G. Willim, and H. Witala, Nucl. Phys. A339, 353 (1980).

[14]G. R. Satchler and W. G. Love, Phys. Rep. 55, 185 (1979).

[15]G. R. Satchler, Nucl. Phys. A279, 61 (1976).

[16]G. R. Satchler, Nucl. Phys. A329, 233 (1979).

[17]F. Todd Baker (private communication).

[18]D. L. Hendrie, Phys. Rev. Lett. 31, 478 (1973).

[19]W. J. Thompson and J. S. Eck, Phys. Lett. 67B, 151 (1977).

[20]T. R. Ophel and A. Johnstron, Nucl. Instrum. Methods. 157, 461 (1978).

[21]P. Braun-Munzinger, G. M. Berkowitz, T. M. Carmier, C. M. Jachcinski, J. W. Harris, J. Barrette, and M. J. Levine, Phys. Rev. Lett. 38, 944 (1977).

[22]M. R. Clover, R. M. DeVries, R. Ost, N. J. A. Rust, R. N. Cherry, Jr., and H. E. Gove, Phys. Rev. Lett. 40, 1008 (1978).

[23]J. G. Cramer, R. M. DeVries, D. A. Goldberg, M. S. Zisman, and C. F. Maguire, Phys. Rev. C 14, 2158 (1976).